Enhanced antimicrobial activity and reduced water absorption of chitosan films graft copolymerized with poly(acryloyloxy)ethyltrimethylammonium chloride

Mohammad Mahbubul Hassan*

Food and Bio-based Products Group, AgResearch Limited, Cnr springs Road & Gerald Street, Lincoln, Christchurch 7647, New Zealand.

ABSTRACT

Chitosan shows selective antimicrobial activity as a bioactive polymer. In this work, a quaternary ammonium derivative of chitosan was synthesized by graft-copolymerization of chitosan with poly[2-(acryloyloxy)ethyltrimethylammonium chloride] or pATC by the redox polymerization method to enhance chitosan's antimicrobial activity. The structural characterizations of the quaternized chitosan were confirmed by Fourier transform infrared spectroscopy, and also by ^{1}H and ^{13}C nuclear magnetic resonance spectroscopy. The produced chitosan was converted into films by solution casting. The physicomechanical properties of the modified chitosan were

* Corresponding author. Tel.: +64-3-321-8755; fax: +64-3-321-8811

E-mail address: mahbubul.hassan@agresearch.co.nz (M.M.Hassan)

compared with the unmodified chitosan. Thermal stability of the films was characterized by thermogravimetric analysis. The pATC grafted chitosan films showed lower thermal stability, water absorption, swelling ratio, and tensile strength compared to the unmodified chitosan film. Antimicrobial activity of the quaternized chitosan was tested against three kinds of bacteria (S*taphylococcus aureus*, *Klebsiella pneumoniae*, and *Pseudomonas aeruginosa*) and two fungi (*Aspergillus brasiliensis* and *Aspergillus fumigatus*). The unmodified chitosan showed good antibacterial activity but no resistance against any fungus. However, the pATC grafted chitosan showed enhanced antibacterial activity against all bacteria investigated. The fungicidal test shows that the pATC-grafted-chitosan showed higher activity against the tested fungi (*Aspergillus fumigatus* and *Aspergillus brasiliensis*) compared to the unmodified chitosan, especially against *Aspergillus fumigatus*.

Keywords: quaternary ammonium chitosan; graft-copolymerization; antimicrobial properties

1. Introduction

Chitosan or poly-(b-1/4)-2-amino-2-deoxy-D-glucopyranose is a natural cationic polysaccharide biopolymer produced from chitin by partial or full deacetylation. Chitin is the second most abundantly available polysaccharide in nature and is the main constituent of the outer skeleton of insects and crustaceans including shrimp, crab and lobster and also the pens of squid. A small percentage of chitin is also found in the outer skin of mushrooms. Structurally chitin resembles cellulose with one hydroxyl group at the C2 position of each glucose unit substituted with an acetyl amine. Chitosan is manufactured from chitin through deacetylation in

sodium hydroxide solution in an inert environment. Chitosan is insoluble in water but soluble in acetic acid solution at below its pKa (6.3) as at that condition the amino groups of chitosan are protonated converting them into NH_3^+ and thereby making them temporarily soluble.

The recent findings of the bioactivity of chitosan resulted in an increased investigation of chitosan for food and biomaterial applications as it is a natural, renewable, and fully biodegradable non-toxic polymer [1,2]. The non-toxicity of chitosan to mammals widens its application as a dietary supplement [3] to textiles [4,5], foods [6], pharmaceuticals [7], cosmetics [8], and water treatments [9,10]. Chitosan and water-soluble chitosan derivatives draw much attention recently as a hydrogel [11,12], cathode interlayer for organic solar cells [13], intestinal inflammation reducer [14], antimicrobial and antifungal agent [15-17], and also as a flame-retardant in thermoplastic polyurethane [9]. It also has been investigated for the controlled delivery of various drugs [18-20], blood anticoagulant [21], immobilization of protein drugs [22], and also as an adsorbent for the removal of heavy metals and metalloids [22–24]. Antibacterial and antifungal properties of chitosan of different molecular weights are well-studied [25,26]. It was found that a decrease in the molecular weight of chitosan increases its solubility in water as well as increasing its antibacterial activity. However, the antimicrobial activity of chitosan is very limited. As the antimicrobial performance of chitosan film is not high, therefore it is blended or graft-copolymerized with other polymers to enhance its antimicrobial activity. In culture media, chitosan has an antimicrobial effect on bacteria (e.g. *Staphylococcus aureu*s, *Listeria monocytogenes*, *Pseudomonas aeruginosa*, *Escherichia coli*, *Shigella dysenteriae* and *Vibrio cholera)* [27,28], and fungi (*Sclerotinia sclerotium*, *Botrytis cinerea*, *Monilinia fructicola*, and *Rhizopus stolonifera*) [29,30]. However, its antimicrobial activity can be affected by the change in the testing conditions. It was reported that when sorbitol was used as a plasticiser in

making chitosan film, it was found that its antifungal performance against *Aspergillus niger* considerably reduced [25].

Chitosan's bioactivity is only limited to acidic conditions as at low pH it shows water solubility. To enhance its water solubility and bioactivity, quaternization, carboxymethylation, sulfation, introducing sulfobetaine and quaternary ammonium, quaternization with phosphonium salt, grafting with ε-poly-L-lysine and modification with coumarin have been investigated [31–36]. Quaternization of chitosan is the most investigated method to make chitosan soluble in water at a wider pH range to widen its applications. The quaternization is usually carried out either by the direct quaternization of amino groups of chitosan or by covalent binding quaternary ammonium compounds, such as of chlorohydroxypropyltrimethylammonium chloride and glycidyl trimethyl ammonium chloride, to the amino groups of chitosan [37,38]. It was reported that the synthesis of a new chitosan derivative by the N-selective introduction of quaternary ammonium-type side chains without the protection of hydroxyl groups [39]. However, the direct quaternization of the amino group of chitosan using alkyl halides under alkaline conditions introduced alkyl groups not only to the amino group but also to the hydroxyl groups.

It is known that the antimicrobial activity of chitosan is affected by the intensity of the positive charge in the macromolecular chain, which can be increased by increasing the number of quaternary ammonium groups in the macromolecular chain of chitosan. By grafting quaternary ammonium polymers, the positive charge density of chitosan can be considerably increased. However, derivatization of chitosan by grafting quaternary ammonium polymer onto the chitosan macromolecular chains have been rarely considered. In this work, a quaternary ammonium polymer, poly(acryloyl)oxyethyltrimethylammonium chloride, was grafted onto chitosan to make a quaternary ammonium derivative of chitosan. Chitosan and chitosan

derivatives were characterized by ^{1}H and ^{13}C NMR, and also by EDX and FTIR. The antimicrobial and antifungal properties of the chemically modified chitosan were carried out by the standard methods. The chitosan derivatives were formed into films and their structure-property relationship was investigated.

2. Materials and procedures

2.1. Materials

Chitosan produced from crab shells with a molecular weight of 190-375 kDa and 75% deacetylated was purchased from Sigma-Aldrich Chemicals (USA). 2-(acryloyloxy)ethyl-trimethylammonium chloride (ATC) monomer and other chemicals (acetic acid and potassium persulfate) were purchased from also Sigma-Aldrich Ltd. All chemicals were used without any further purification except 2-(acryloyloxy)ethyltrimethylammonium chloride, which was purified by column separation to remove the added polymerization inhibitor, monomethyl ether hydroquinone. The cultures of bacteria (*Staphylococcus aureus, Klebsiella pneumoniae,* and *Pseudomonas aeruginosa*), and fungi (*Aspergillus fumigatus* and *Aspergillus brasiliensis*), were procured from Environmental Science Research (ESR) of New Zealand.

2.2. Synthesis of pATC-grafted Chitosan

The grafting of pATC onto chitosan macromolecular chain was carried out by the redox polymerization at 25 °C. 1.5 g chitosan was dissolved in 75 ml of 1% acetic acid solution. The insoluble admixtures in chitosan solution were separated by centrifuging at 4000 rpm for 5 minutes. The admixture-free chitosan solution was decanted and was taken in a 500 ml size three neck conical flask. The solution was purged with nitrogen for 30 min and the flask was placed in a glycerin bath. An appropriate amount (30 and 50% on the weight of chitosan) of ATC monomer diluted in water was added to it drop-wise with high-speed stirring and continuous purging with nitrogen. When the addition was completed, the reaction was kept under agitation at room temperature for 6 h under nitrogen environment. An appropriate quantity of potassium peroxydisulfate (5% of the weight of monomer) was then added with stirring and then pre-dissolved ferrous sulfate solution was added (the ratio peroxidisulfate to ferrous sulfate was 20:1). The polymerization reaction was continued for 2 h. The viscosity of chitosan solution decreased due to the grafting of poly(2-acryloyloxy)ethyltrimethylammonium chloride (pATC), which increased the solubility of chitosan in water. The pATC-grafted chitosan was then cooled to room temperature and poured into Petri dishes. The solvent was evaporated by placing them in a fume hood and films of PATC-g-chitosan were collected for further characterizations. The film of unmodified chitosan was also produced in the same manner by dissolving in 1% acetic acid solution using the same concentration of chitosan. The chitosan grafted with 30 and 50% pATC is denoted here as CS-pATC-30 and CS-pATC-50 respectively. The mechanism of grafting of pATC onto the macromolecular chain of chitosan is shown in Fig. 1.

2.3. Formation of chitosan films

The films of chitosan, CS-pATC-30, and CS-pATC-30 were prepared by an aqueous solvent casting method. Aqueous solutions of chitosan and pATC grafted chitosan were poured on rectangular plastic-made Petri dishes and the water was evaporated by placing them under a fume hood. The unmodified chitosan film was almost colorless and transparent but the pATC grafted chitosan films were slightly golden yellowish color. The thickness of the produced films was quite uniform.

2.4. Nuclear magnetic resonance

Dilute solutions of chitosan, CS-pATC-30 and CS-pATC-50 were prepared by adding 70 mg of the samples in D_2O/CD_3COOD mixture at around pH 4. Nuclear magnetic resonance was used to confirm the polymeric grafting The ^{1}H NMR and ^{13}C NMR spectra of unmodified and pATC grafted chitosan were recorded on a Varian 600 MHz NMR (Model: VNMRS 600, Varian Inc., Palo Alto, USA). The chemical shifts were expressed in ppm downfield of tetramethylsilane (TMS) as an internal standard. The calculation of the degree of quaternization of chitosan from 1H-NMR spectra was based on the ratio between the peak integration of the protons from the quaternary ammonium groups 3.1 ppm and from the methyl group in residual acetyl groups of chitosan at 1.8 to 1.9 ppm.

2.5. Physical characterization

The chitosan films were cut in 1×1 cm size and they were then dried under vacuum for a week. After taking the initial weight (W_0) of the films, they were then soaked in 50 ml of MiliQ water for three days. After which the films were removed, excess water was wiped out with a blotting tissue paper and weighed again (W_3). The swelling ratio of the various chitosan films was assessed by the following formula:

$$Swelling\ ratio\ (\%) = \frac{W_3 - W_0}{W_0} \times 100 \qquad [1]$$

Water vapor permeability of chitosan films was measured by the gravimetric method by placing 24 ml of water in a glass vial and chitosan film was placed on top of the vial according to ISO 2528 standard method (1995(E) [40]. The vials were then tightly sealed with a screw cap having a round-shape opening. The Water Vapour Transmission Rate (WVTR) of films was determined by the following formula:

$$WVTR\ (g/m^2) = \frac{W_o - W_t}{A} \times 1000000 \qquad [2]$$

where W_o and W_t are the weight of water (g) at time zero and t respectively and A is the area of the film (mm^2).

The water absorption of films was carried out by 172 h immersion method according to ASTM D570: *Standard Test Method for Water Absorption of Plastics*. KSV CAM 200 Contact Angle Measurement Apparatus (made by KSV Instruments, Finland) was used to measure the contact angle. The contact angle calculation was performed by applying the spherical approximation of the drop by curve fitting based on the Young-Laplace equation by using the software (KSV CAM 200) supplied with the equipment.

The transparency of the film was measured by a Thermo Scientific UV-vis spectrometer (Model: Evolution 220, Thermo Electron Scientific Instruments LLC, Madison, USA) using the transmission mode. The *CIE L*a*b** color of the unmodified and pATC grafted chitosan films were measured by a Mahlo hand-held reflectance spectrophotometer (Model: Color-guide 45/0, Mahlo GmbH & Co. KG, Saal/Donau, Germany) underD65 illuminant and 10° observer. At least three replicates were tested for each chitosan sample and the averages are reported here.

2.6. Mechanical and chemical characterization of chitosan films

The thickness of various chitosan films was measured by a Mitutoyo digital slide caliper (Mitutoyo Corporation, Japan). Five thickness values were taken along the length of the filmstrip and the average value was used for tensile strength calculation. The tensile strength and elongation properties of the ordinary chitosan and PATC-g-chitosan films were assessed by using an Instron Universal Tensile Testing Machine (Model 4204) at 20±2 ºC and 65±2% relative humidity according to the ASTM Test Method D882 - 2: *Standard Test Method for Tensile Properties of Thin Plastic*. The sample size was 25 × 70 mm, the gauge length was 50 mm and the crosshead speed was 50 mm/min. The samples were conditioned at the above-mentioned temperature and humidity for 3 days prior to testing.

2.7. Thermogravimetric analysis

Thermogravimetric (TG) analysis is a useful tool to evaluate the thermal stability of polymers. An atmospheric pressure thermogravimetric analyzer (TGA) Model SDT Q600 made

by TA Instruments (New Castle, USA) was used to assess the thermal stability of unmodified and pATC grafted chitosan. All TGA runs employed nitrogen (99.99% pure and food-grade) as the purge gas for the furnace with a constant flow rate of 100 ml/min. For each run, 7−10 mg of chitosan and pATC grafted chitosan samples were loaded in a platinum pan. The samples were heated to 800 °C at the rate of 10 °C/min under a constant nitrogen gas flow (100 ml/min). The sample was then held for a further 10 min at the pyrolysis temperature and slowly cooled down to room temperature by switching off the furnace.

2.8. *Scanning electron microscopy*

The morphology of the chitosan films was investigated using SEM techniques. The surface of chitosan films was scanned using a Hitachi SEM (Model: TM3030 Plus, Hitachi Corporation, Japan) with an accelerated voltage of 15 kV without any conductive coating. The energy dispersive spectra (EDX) were recorded using the same instrument with a Quantex75 EDX attachment.

2.9. Assessment of antibacterial and antifungal properties

The antibacterial properties of chitosan and pATC grafted chitosan were assessed by a qualitative method according to the AATCC Test Method 147-1998. In this method, 1 ml of 24 hour broth culture of bacteria is mixed with 9 ml of sterile distilled water in a Petri dish and one loopful of diluted inoculum is transferred to the surface of the sterile agar plate by making five streaks, approximately 60 mm in length and spaced 10 mm apart covering the central area of a

standard Petri dish. A thick layer of gel of unmodified chitosan as well as chitosan grafted PATC was gently poured transversely across the inoculum streak to ensure intimate contact with the agar plate and incubated at 37±2 °C for 24 h, after which the interruption of bacterial growth along the streaks of inoculum under the specimen and zone of inhibition beyond its edge are examined. No growth of bacteria under the tested samples and also showing a zone of inhibition provides an indication of antimicrobial performance. The bacteria used were *Staphylococcus aureus* (ATCC 6538), *Klebsiella pneumoniae* (ATCC 4352) and *Pseudomonas aeruginosa* (NZ isolate ARL09/165).

Antifungal properties of unmodified and modified chitosan were assessed according to ISO 16869-2001: *Plastics - Assessment of the effectiveness of fungistatic compounds in plastics formulations*. For this method, 3.8±0.5 cm diameter disk-shaped samples were cut from casted films of chitosan and CS-pATC-50. The fungi used were *Aspergillus fumigatus* (ATCC 1022), and also a mixture of *Aspergillus brasiliensis* (ATCC 16404) and *Aspergillus fumigatus* (ATCC 1022). The culture medium was comprised of 3 g/l ammonium nitrate, 2.5 g/l potassium dihydrogen phosphate, 2 g/l dipotassium hydrogen phosphate, 0.2 g/l magnesium sulfate, 0.1 g/L ferrous sulfate and 20 g/l agar. Three replicates for each sample were carried out and the results were averaged. All data were presented as the means ± SD of three independent measurements and submitted to variance analysis (ANOVA) using SPSS software (version 18.0 for Windows, SPSS, Inc., Chicago, IL, USA. Statistical differences were considered to be significant at $p < 0.05$.

3. Results and discussion

3.1. Quaternization of chitosan by grafting with pATC.

The graft-copolymerization of chitosan with pATC was confirmed by comparing the FT-IR, NMR, and EDX spectra of neat chitosan and pATC-grafted chitosan synthesized by using two different concentrations of ATC monomer. The FT-IR spectra of unmodified chitosan, CS-pATC-30, and CS-pATC-50 are presented in Fig. 2. The spectrum of unmodified chitosan shows characteristics bands of glucosamine. The strong broad peak at around 3200 cm^{-1} could be attributed to the hydroxyl groups. The bands at 2878 and 2927 cm^{-1} could be attributed to the $–CH_2–$ and $–CH_3$ stretching the vibrations respectively. The band at 1635 cm^{-1} could be assigned to the N–C bending vibration. The bands at 1634 and 1540 cm^{-1} could be attributed to the carbonyl stretching vibrations of amide I and amide II groups in chitosan respectively [41]. On the other hand, the spectra of CS-pATC-30 and Cs-pATC-50 show new bands at 952, 1472, and 1732 cm^{-1}. The bands at 952 and 1472 cm^{-1} could be attributed to the stretching vibration of quaternary ammonium and bending vibrations of methyl groups of quaternary ammonium moieties respectively [42]. The very intense new band formed at 1732 cm^{-1} is due to the stretching vibration of C=O present in the grafted pATC. It can be seen that the band at 1634 cm^{-1} of the unmodified chitosan moved to 1650 cm^{-1} for the pATC-grafted chitosan. On the other hand, the intensity of the hydroxyl peak at 3200 cm^{-1} is almost unchanged for the unmodified and pATC-grafted chitosan indicating that pATC mainly grafted with the amino groups of chitosan. All the above-mentioned characteristic peaks are showing evidence that the chitosan and pATC were graft-copolymerized.

Chitosan has three reactive functional groups, such as the primary amino (C-2), primary hydroxyl (C-6) and secondary hydroxyl (C-3) groups and all of them are nucleophilic. The amino group is mainly responsible for the physicochemical properties of chitosan at pH below 6.5 [43].

The NMR technique is used to accurately assess the chemical structure of organic and polymeric materials. Fig. 3 represents the ^{1}H NMR spectra of unmodified chitosan and CS-g-pATC-50. The signals shown in the spectrum of chitosan are consistent with those previously reported in the literature [43,44]. The signals observed for the spectrum of unmodified chitosan at various ppm can be associated with (1) δ = 0.9 ppm (–CH_2–), δ = 1.97 ppm (N-acetyl), δ = 2.1 ppm (N–H), δ = 2.97 ppm (H2), δ = 3.53–3.56 ppm (H5, H6), δ = 4.79 ppm (H3, H4), δ = 4.62 ppm (H1). In contrast the ^{1}H NMR spectrum of CS-g-pATC shows signals at δ = 1.12 ppm [$(CH_2)_4$], δ = 1.92 (N-acetyl), δ = 2.27 ppm (H9, H10), δ = 2.99 ppm (H8, –$N^+(CH_3)_3$ group), δ = 3.08 ppm [$N(CH_3)_3^+$], δ = 3.22 ppm (H7), δ = 3.36 (three equivalent methyl groups of ammonium), δ = 3.63 ppm (H5), δ = 3.65 ppm (–N^+–C*H*$_2$–CH_2–O–), δ = 3.73 (H8) and δ = 4.49 ppm (H1). The NMR spectra confirm that pATC was successfully grafted onto chitosan.

The ^{13}C NMR spectra of the unmodified and 50% pATC grafted chitosan are shown in Fig. 4. The signals shown by the spectrum of unmodified chitosan can be interpreted as: δ = 97.57 ppm (C1), δ = 76.24 ppm (C4), δ = 74.69 ppm (C5), δ = 69.78 ppm (C3), δ = 60.00 ppm (C6), δ = 57.34 and 54.00 ppm [$^{+}N(CH_3)_3$], δ = 55.71 ppm (C2). The spectrum of CS-g-pATC-50 also shows similar signals, δ = 97.80 ppm (C1), δ = 76.28 ppm (C4), δ = 74.72 ppm (C5), δ = 70.29 ppm (C3), δ = 60.00 ppm (C6), δ = 55.59 ppm (C2). The spectrum of CS-g-pATC-50 also shows new signals at δ = 180.7 ppm (C=O), δ = 133 ppm [(–C–C) –], δ = 127 ppm [alkenes or $(–CH_2)_2$], δ = 64.5 ppm (methylene carbon), δ = 58.32 ppm $[CH_3)_3N^+]$, and δ = 54 ppm (C10) are visible. These data show that pATC has been successfully grafted onto chitosan.

Table 1 shows elemental analysis of unmodified chitosan, CS-pATC-30 and CS-pATC-50 showing the composition of C, O, N, and Cl. It can be seen that C, O, N, and Cl content of unmodified chitosan are 52.71, 38.38, 8.91 and 0 respectively. In the case of chemically modified

chitosan, Cl content increased with an increase in the applied concentration of ATC monomer. The decrease in O content with an increase in the pATC weight% suggests that pATC grafted onto chitosan by reacting with its hydroxyl groups. The calculation of the degree of quaternization indicates that the degree of quaternization for the CS-pATC-30 and CS-pATC-50 is 0.18 and 0.35 respectively.

The degree of quaternization of chitosan depends on the reaction time, temperature, initiator concentration and also the molar ratio between chitosan and the ATC. In this work, the quaternization of chitosan was carried out at pH 4 and only the concentration of ATC monomer was varied. At acidic conditions, the primary and secondary hydroxyl groups are not sufficiently nucleophilic but the amino groups are nucleophilic at that condition. Therefore, the amino groups are more reactive than the hydroxyl groups at that condition and pATC is mainly grafted to the amino groups of chitosan, which is confirmed by the FTIR and NMR spectral analysis.

3.2. Mechanical properties

Despite chitosan's attractive biological properties, concerns regarding the material's low strength and brittle behavior limit its use for various applications. Table 2 shows the tensile strength of unmodified chitosan and pATC grafted chitosan films hydrated at standard atmospheric conditions for two days. The unmodified chitosan film showed quite good tensile strength, much higher than the tensile strength reported by others [11,40], as they are made from various insects and crustaceans with a range of molecular weights. It can be seen that the tensile strength of chitosan decreased and its peak elongation increased with an increase in the pATC

weight%. The unmodified chitosan film showed tensile strength 21.16±1.82 MPa, which decreased to 15.26±0.30 and 10.06±1.08 for the CS-pATC-30 and CS-pATC-50 respectively. Similarly, the breaking strength also decreased with an increase in the concentration of ATC monomer. Although the grafting with pATC reduced the tensile strength of chitosan, the films still had reasonably good tensile strength. It is evident that the grafting of chitosan with pATC considerably decreased the elasticity of the of the chitosan film as the grafted films showed lower elongation compared to the unmodified chitosan film. For the CS-pATC-50 film, the peak elongation was almost double of the peak elongation shown by the unmodified chitosan. The low elongation showed by the grafted chitosan films suggests that the brittleness of the chitosan film considerably increased after grafting with pATC.

Fig. 5 represents the stress-strain curve of unmodified chitosan film as well as CS-pATC-30, and CS-pATC-50 films. The most important observation is that the pATC grafted films showed low strain-to-failure compared to the unmodified chitosan film. The strain to failure decreased with an increase in the pATC loading in the chitosan films. The pattern of the stress-strain curve of the CS grafted chitosan films is quite different from the curve of unmodified chitosan film. In the case of unmodified chitosan, the stress increased initially and then decreased with an increase in the strain (%) up to 6% strain, after which became a plateau. On the other hand for the pATC chitosan films, the stress gradually increased with an increase in the strain. The unmodified chitosan showed much higher yield strength compared to the pATC grafted chitosan films as its yield strength was almost double of the yield strength of CS-pATC-50. The results indicate that the grafted pATC polymer had much lower tensile strength compared to the chitosan.

Several researchers reported that in an acidic solution, molecular chain scission of chitosan takes place, which increases with an increase in temperature [45,46]. Molecular chain scission of

chitosan also takes place during grafting by the polymerization initiator. In the case of control chitosan film, chitosan solution was not heated at 60 °c for two hours like pATC-grafted chitosan. Therefore, the control chitosan film showed considerably higher strength than the pATC-grafted chitosan. In the case of elongation at break, the pATC-grafted chitosan had different hydrogen bonding than the neat chitosan as some of the amino groups were replaced with the branching of pATC, which reduced the mobility of the molecular chains, thereby reducing the extensibility of the film.

3.3. Thermal analysis

The thermal decomposition temperature of the unmodified and pATC grafted chitosan films was measured by thermogravimetric analysis. Fig. 6 shows the thermogravimetric and differential thermal analysis curves of chitosan and CS-pATC-50 films. It can be seen that chitosan and CS-pATC-50 films both showed very similar weight loss up to 220 ℃ and also at 450 to 800 ℃. However, from 220 to 450 ℃ CS-pATC-50 showed much higher weight loss compared to the weight loss observed for the unmodified chitosan. The thermogravimetric curve of chitosan shows that chitosan loses its weight mainly at three stages, room temperature to 221 ℃, a rapid weight loss at 221 to 400 ℃ and very slow weight loss from 385 to 800 ℃, which is consistent with the weight loss observed by others [47]. The weight loss of approximately 20% at room temperature to 221 ℃ took place due to the loss of volatiles (the moisture absorbed into chitosan and held by hydrogen bonding with amino and hydroxyl groups of chitosan). In the second stage, the major weight loss occurred (approx. 40%) at 221 to 400 ℃, and is due to the

thermal degradation of chitosan, i.e. depolymerization/decomposition of polymer chains through deacetylation and cleavage of glycosidic linkages [48]. In the last stage, a small weight loss was observed from 400 to 800 °C is due to the thermal destruction of pyranose ring and the decomposition of the residual carbon [49]. In the DTA curves, unmodified chitosan showed two peaks, a small peak at 119 °C and a large peak at 257 °C. It means that the peak thermal degradation temperature of chitosan is 257 °C. In the case of CS-pATC-50 the weight loss also occurred at three stages but at different temperature regions, room temperature to 214 °C, 214 to 328 °C and 328 to 800 °C. The DTA curves of CS-pATC-50 showed three peaks, two small peaks at 114 and 239.7 °C and a large peak at 250 °C. The weight loss at 114 °C is due to the loss of moisture, but the 239.7 and 250 °C is due to the depolymerization/degradation of grafted pATC, and due to the thermal degradation of chitosan. The TG data shows that the grafting of pATC to chitosan affected the thermal stability of chitosan from 214 to 328 °C but not the overall thermal stability as the ash content of chitosan and pATC grafted chitosan at 500 to 800 °C was exactly same. It indicates that the grafted pATC was totally degraded at 500 °C. The peak degradation temperature decreased for the CS-pATC-50 (250°C) compared to peak degradation temperature of chitosan (257 °C), indicating that pATC was successfully grafted to chitosan.

3.4. Contact angle

Table 3 shows contact angle of the surface of unmodified chitosan and also chitosan grafted with pATC with 30 and 50% pATC loading up to 120 s at 30 s intervals. It is evident that

modified and unmodified both types of chitosan films showed some levels of hydrophilicity. The contact angle of unmodified chitosan film immediately after placing the water droplet was 87.9°, which decreased to 81.2° after 30 s. After which the contact angle became quite steady up to 120 s. On the other hand, pATC grafted chitosan immediately after placing the water droplet showed slightly higher contact angle than the contact angle shown by the unmodified chitosan film but the contact angle gradually decreased with time. In the case of CS-pATC-30 contact angle decreased to 74.5° at 120 s but CS-pATC-50 showed similar contact angle at 60 s of the test and at 120 s decreased to 68.8°. The results suggest that the hydrophilicity of chitosan film increased with pATC loading in the chitosan films. Before the formation of the film by evaporation, the grafted chitosan derivatives showed better water solubility and lower viscosity compared to the unmodified chitosan but after the formation of the film by evaporation, their solubility decreased. Probably the grafted chitosan film had higher van der Waals bonding due to the evaporation of water compared to the unmodified chitosan, which blocked the hydrophilic groups resulting in a decrease in the water absorption by the grafted chitosan films.

3.5. Transparency of chitosan films.

Fig. *S1* (Supplementary Content) shows the transparency of the unmodified chitosan, and also chemically-modified chitosan films. It can be seen that the unmodified chitosan film shows excellent transparency at 427 to 541 nm as the transmittance of the light through the unmodified chitosan film at that wavelengths are almost 100%. On the other hand, CS-pATC-30 and CS-pATC-50 show transparency only 424–493 and 436–492 nm wavelengths. The pATC grafted

chitosan films show an absorption peak at 510 nm and its intensity increased with an increase in the concentration of ATC monomer as the grafted films were slightly golden yellow in color compared to the colorless chitosan film. The CIE L*a*b* color values of unmodified, CS-pATC-30 and CS-pATC-50 chitosan films are shown in Table S1 (Supplementary content), where L*, a*, and b* represents lightness to darkness, red to green and blue to yellow respectively. It can be seen that value of L*, a* and b* values increased with an increase in the pATC weight% in the pATC-grafted chitosan. The lowest value was shown by the control chitosan and the highest value by the CS-pATC-50. The yellowness and redness of chitosan films increased with an increase in the in the pATC weight%.

3.6. *Water vapor transmission rate.*

The WVTR of a plastic film indicates its ability to transmit water vapor through the film, which is useful in predicting the in-service performance of that plastic film. Fig. 7 shows the WVTR of unmodified and grafted chitosan films up to 172 h. It can be seen that at the initial 24 h of the test, the pATC-grafted chitosan films showed considerably lower WVTR compared to the unmodified chitosan film and the WVTR decreased with an increase in the weight% of pATC in the pATC-grafted chitosan films. After 2 h test, the CS-pATC-30, and CS-pATC-50 films showed WVTR 24.8 and 15.6 g/m^2, compared to the WVTR shown by the control chitosan film, which shoed WVTR 12.0 g/m^2. The Cs-pATC-50 showed 51.6% lower WVTR compared to the WVTR showed by the unmodified chitosan film. The WVTR of unmodified and pATC-grafted chitosan films increased with an increase in time. At 24 h, the WVTR for CS-pATC-30, and CS-

pATC-30 films were 456.2, 44.6 and 425.4 g/m^2 respectively. However, after 48 h test, the WVTR of all unmodified and pATC grafted chitosan films became almost similar, which continued up to the end of the 172 h study. Therefore, we can conclude that up to 24 h study, the grafted films showed considerably lower WVTR compared to the WVTR shown by the unmodified chitosan film but after 48 h study, all the tested films showed quite similar WVTR indicating that the grafting of chitosan with pATC does not change its WVTR.

3.7. Swelling ratio

Table 2 shows the swelling ratio of unmodified and pATC grafted chitosan films. The grafting of pATC onto chitosan considerably reduced chitosan's swelling ratio. After three days of the test, the unmodified chitosan film disintegrated into several pieces but the pATC grafted films were fully intact. The swelling ratio of unmodified chitosan film was 3497%, which considerably decreased after grafting with the pATC. However, the swelling ratio increased with an increase in the weight% of pATC. The swelling ratio of CS-pATC-30 and CS-pATC-50 was 534 and 880% respectively. The results indicate that the moisture absorbency of chitosan is greatly affected by the introduction of the hydrophobic long alkyl chain of pATC, although at the end of the hydrophobic chain there are hydrophilic quaternary ammonium groups.

3.8. Water absorption

Fig. *S2* (Supplementary Content) shows water absorption vs time curves of untreated and pATC grafted chitosan films. It is evident that the water absorption capacity of chitosan overwhelmingly decreased after grafting with pATC. The water absorption rate for the unmodified chitosan film was very high and within 15 min reached 8571.6% and then started to going down as the disintegration and dissolution of the film started to take place. It was not possible to measure the water absorption capacity after 20 minutes of soaking as the film disintegrated. On the other hand, CS-pATC-30 film showed very low water absorption and showed the highest absorption (140.6%) at 30 min of soaking. After which slightly decreased to 136.8% and was almost stable up to 140 min of soaking. The chitosan film did not disintegrate even after three days of soaking. The CS-pATC-50 film also showed similar behavior but showed considerably higher water absorption compared to the water absorption shown by the CS-pATC-30 but not comparable to the unmodified chitosan film. The CS-pATC-30 and CS-pATC-50 both showed rapid water absorption within 5 min of soaking but the former reached to the highest water absorption level at 30 min of soaking but the latter reached at the highest water absorption capacity at 90 min of soaking and the maximum water absorption (%) was 251.7%, almost double of the water absorption capacity shown by the CS-pATC-50 film. It also started to disintegrate after 140 min of soaking in water.

3.9. Surface morphology

The microstructure of surface of films depends on the presence of other components (e.g. acetic acid) and also the drying conditions. SEM images of unmodified chitosan, CS-pATC-30,

and CS-pATC-50 films are shown in Fig. *S3* (Supplementary Content). It is evident that the surface of unmodified chitosan film is quite smooth and produced a compact structure. The surface of CS-pATC-30 film was also smooth, similar to the unmodified chitosan film. On the other hand, CS-pATC-50 films produced micro-wrinkles. Probably the grafting of pATC caused uneven shrinkage of the film during drying.

3.10. Antimicrobial properties

Antibacterial properties of unmodified chitosan film, CS-pATC-30 and CS-pATC-50 are shown in Table 4. The unmodified and pATC grafted chitosan films all showed quite good antibacterial performance against all bacteria investigated. However better activity was observed against *Staphylococcus aureus* and *Pseudomonas aeruginosa* than the *Klebsiella pneumoniae*. In the case of all unmodified and modified chitosan films, no growth of bacteria was seen under or on the chitosan films for all the bacteria. In the case of *Pseudomonas aeruginosa*, the first bacterial streak showed 1-2 mm zone of inhibition but other streaks showed more than 5 mm zone of inhibition. On the other hand, CS-pATC-30 film showed 1mm zone of inhibition for all the streaks and size of zone inhibition increased to 1-2 mm for the CS-PATC-50 film. In the case of *Staphylococcus aureus*, the unmodified chitosan film showed excellent antibacterial activity as the size of the zone of inhibition was 10 mm or more. For the first two bacterial streaks, both grafted chitosan films showed 1-2 mm zone of inhibition and for the rest of the streaks, the size of the zone of inhibition was similar to the unmodified chitosan. The antibacterial activity of chitosan films against *Klebsiella pneumoniae* is quite interesting. For the first two bacterial

streaks, no zone of inhibition was observed in the case of unmodified chitosan and Cs-pATC-30 films but 5 mm zone of inhibition was seen around the fabric for first and second streaks and 5 mm for the third to 5^{th} streaks. The results indicate that the antibacterial activity of chitosan against *Klebsiella pneumoniae* increases with an increase in the percentage of grafted pATC. The decrease in the size of the zone of inhibition indicates that the solubility of chitosan decreased after the graft copolymerization with pATC, which reduced leaching of chitosan to the solution. The non-grafted chitosan diffuses to the surroundings and increases the size of the zone of inhibition but the grafted chitosan is slowly released to the surroundings causing the small size of the zone of inhibition. In summary, the grafting of pATC to chitosan increased chitosan's overall antibacterial activity

Fig. 8 shows the antifungal activity of unmodified chitosan, CS-pATC-30, and CS-pATC-50 films after 2 and 14 days of incubation with *Aspergillus fumigatus,* and also a mixture of *Aspergillus fumigatus* and *Aspergillus brasiliensis*. It can be seen that unmodified chitosan film did not show any antifungal activity against no fungi and dense fungi population can be seen growing on the chitosan film for both the fungi. On the other hand, CS-pATC-50 showed some levels of inhibition of growth of *Aspergillus brasiliensis* but excellent inhibition of growth of *Aspergillus fumigatus*. Overall, pATC grafted chitosan showed better antimicrobial activity compared to the antimicrobial activity shown by the unmodified chitosan.

4. Conclusions

A quaternary chitosan derivative has been synthesized by grafting pATC onto chitosan macromolecular chains by redox polymerization. FTIR, EDX and NMR characterizations confirm that pATC successfully grafted onto chitosan. The grafted chitosan film showed considerably lower swelling ratio, tensile strength, strain-to-failure and also lower water absorption compared to the unmodified chitosan. The tensile strength of the chitosan films decreased with an increase in the weight% of pATC. Unmodified chitosan showed good antibacterial activity against all three bacteria but very poor activity against the two fungi investigated in this work. The pATC grafted chitosan showed excellent antibacterial activity against the all three bacteria and also against *Aspergillus fumigatus* fungi but some level of activity against *Aspergillus brasiliensis*. The developed chitosan films may find applications as antimicrobial patches, wound dressings, and food packaging.

Conflicts of interest

The author would like to declare that no financial interest.

Acknowledgment

The authors acknowledge the financial support received from the Ministry of Business, Innovation, and Employment (MBIE) of the New Zealand Government through Grant No. C10X0824. The author would like to thank Barbara Müller (RJ Hill Laboratories Ltd.) and Malik Altaf Hussain (Lincoln University) for the assessment of antibacterial and antifungal performance respectively.

References

[1] H.D.M. Follmann, A.F. Naves, A.F. Martins, et al., Advanced fibroblast proliferation inhibition for biocompatible coating by electrostatic layer-by-layer assemblies of heparin and chitosan derivatives, J. Colloid Interf. Sci. 474 (2016) 9–17.

[2] Y.-W. Jiang, H.-Y. Guo, Z. Chen, Z.-W. Yu, et al., In situ visualization of lipid raft domains by fluorescent glycol chitosan derivatives. Langmuir 32 (2016) 6739–6745.

[3] C. Ni Mhurchu, S.D. Poppitt, A.-T. McGill, et al., The effect of the dietary supplement, chitosan, on body weight: A randomized controlled trial in 250 overweight and obese adults, Int. J. Obesity 28 (2004) 1149–1156.

[4] S.-H. Lim, S.M. Hudson, Application of a fiber-reactive chitosan derivative to cotton fabric as an antimicrobial textile finish, Carbohyd. Polym. 56 (2004) 227–234.

[5] F. Ferrero, M. Periolatto Antimicrobial finish of textiles by chitosan UV-curing, J. Nanosci.Nanotechnol. 12, (2012). 4803–4810.

[6] R.A.A. Muzzarelli, Chitosan-based dietary foods, Carbohyd. Polym. 29 (1996) 309–316.

[7] L. Illum, Chitosan and its use as a pharmaceutical excipient, Pharmaceut. Res. 15 (1998) 1326–1331.

[8] A. Jimtaisong, N. Saewan Utilization of carboxymethyl chitosan in cosmetics, Int. J. Cosmet. Sci. 36 (2014) 12–21.

[9] X. Liu, X. Gu, J. Sun, S. Zhang, Preparation and characterization of chitosan derivatives and their application as flame retardants in thermoplastic polyurethane, Carbohydr. Polym. 167 (2017) 356–363.

[10] F.A. Bertoni, J.C. Gonzälez, S.I. García, et al., Application of chitosan in removal of molybdate ions from contaminated water and groundwater, Carbohydr. Polym. 180 (2018) 55–62.

[11] Y. Chen, F. Wang, N. Zhang, et al., Preparation of a 6-OH quaternized chitosan derivative through click reaction and its application to novel thermally induced/polyelectrolyte complex hydrogels, Colloid. Surf. B 158 (2017) 431–440.

[12] M. Yar, S. Shahzad, L. Shahzadi, et al., Heparin-binding chitosan derivatives for production of pro-angiogenic hydrogels for promoting tissue healing, Mater. Sci. Eng. C 74 (2017) 347–356.

[13] K. Zhang, R. Xu, W. Ge, et al., Electrostatically self-assembled chitosan derivatives working as efficient cathode interlayers for organic solar cells. Nano Energy 34 (2017) 164–171.

[14] H. Hyun, S. Hashimoto-Hill M. Kim, et al., Succinylated chitosan derivative has local protective effects on intestinal inflammation, ACS Biomat. Sci. Eng. 3 (2017) 1853–1860.

[15] W. Tan, J. Zhang, F. Luan, et al., Design, synthesis of novel chitosan derivatives bearing quaternary phosphonium salts and evaluation of antifungal activity. Int. J. Biol. Macromolecule. 102 (2017) 704–711.

[16] N.L. Vanden Braber, L.I. Díaz Vergara, F.E. Morán Vieyra, et al., Physicochemical characterization of water-soluble chitosan derivatives with singlet oxygen quenching and antibacterial capabilities. Int. J. Biol. Macromolecule.102 (2017) 200–207.

[17] M.C. Bonferoni, G. Sandri, S. Rossi, et al., A novel ionic amphiphilic chitosan derivative as a stabilizer of nanoemulsions: Improvement of antimicrobial activity of *Cymbopogon citratus* essential oil, Colloid. Surf. B 152 (2017) 385–392.

[18] H. Hattori, H. Tsujimoto, K. Hase, M. Ishihara, Characterization of a water-soluble chitosan derivative and its potential for submucosal injection in endoscopic techniques, Carbohydr. Polym. 175 (2017) 592–600.

[19] J.-T. Lin, Z.-K. Liu, Q.-L. Zhu, et al., Redox-responsive nanocarriers for drug and gene co-delivery based on chitosan derivatives modified mesoporous silica nanoparticles, Colloid. Surf. B 155 (2017) 41–50.

[20] K. Chen, Y. Ling, C. Cao, et al., Chitosan derivatives/reduced graphene oxide/alginate beads for small-molecule drug delivery, Mater. Sci. Eng. C 69 (2016) 1222–1228.

[21] Y.A. Skorik, A.S. Kritchenkov, Y.E. Moskalenko, et al., Synthesis of N-succinyl- and N-glutaryl-chitosan derivatives and their antioxidant, antiplatelet, and anticoagulant activity, Carbohydr. Polym. 166 (2017) 166–172.

[22] E.-H. Kim, G.-D. Han, J.-W. Kim, et al., Visible and UV-curable chitosan derivatives for immobilization of biomolecules. Int. J. Biol. Macromolecule. 104 (2017) 1611–1619.

[23] M. O. Abd El-Magied, A. A. Galhoum, A. A., Atia, et al., Cellulose and chitosan derivatives for enhanced sorption of erbium(III), Colloid. Surf. A 529 (2017) 580–593.

[23] B. Liao, N. Guo, S.-J. Su, et al., Efficient separation and high selectivity for cobalt and nickel from manganese solution by a chitosan derivative: Competitive behavior and interaction mechanisms, Ind. Eng. Chem. Res. 56 (2017) 3418–3428.

[24] X. Wang, Y. Liu, J. Zheng, Removal of As(III) and As(V) from water by chitosan and chitosan derivatives: a review. Environ. Sci. Pollution Res. 23, (2016) 13789–13801.

[25] A.P. Martínez-Camacho, M.O. Cortez-Rocha, J.M. Ezquerra-Brauer, et al., Chitosan composite films: Thermal, structural, mechanical and antifungal properties. Carbohydr. Polym. 82 (2010) 305–315.

[26] Z. Guo, R. Xing, S. Liu, et al., Antifungal properties of Schiff bases of chitosan, N-substituted chitosan and quaternized chitosan. Carbohydr. Res. 342 (2007) 1329–1332.

[27] M.S. Benhabiles, R. Salah, H. Lounici, et al., Antibacterial activity of chitin, chitosan and its oligomers prepared from shrimp shell waste, Food Hydrocolloid. 29 (2012) 48–56.

[28] V. Coma, A. Deschamps, A. Martial-Gros, Bioactive packaging materials from edible chitosan polymer: Antimicrobial activity assessment on dairy-related contaminants, J. Food Sci. 68, (2003) 2788–2792.

[29] S.J. Jeon, M. Oh, W.-S. Yeo, et al., Underlying mechanism of antimicrobial activity of chitosan microparticles and implications for the treatment of infectious diseases, PLoS One 9 (2014) e92723,

[30] H. Li, T. Yu, Effect of chitosan on incidence of brown rot, quality and physiological attributes of postharvest peach fruit. J. Sci. Food Agricultur. 81 (2001) 269–274.

[31] D. Zhu, H. Cheng, J. Li, et al., Enhanced water-solubility and antibacterial activity of novel chitosan derivatives modified with quaternary phosphonium salt, Mater. Sci. Eng. C, 61 (2016) 79–84.

[32] F.T.R. de Almeida, B.C.S. Ferreira, A.L.S.L. Moreira, et al., Application of a new bifunctionalized chitosan derivative with zwitterionic characteristics for the adsorption of Cu^{2+}, Co^{2+}, Ni^{2+}, and oxyanions of Cr^{6+} from aqueous solutions: Kinetic and equilibrium aspects, J. Colloid Interf. Sci. 466 (2016) 297–309.

[33] G. Yang, Q. Jin, C. Xu, S. Fan, C. Wang, P. Xie, Synthesis, characterization and antifungal activity of coumarin-functionalized chitosan derivatives, Int. J. Biologic. Macromol. 106 (2018) 179–184.

[34] Y. Chen, J. Li, Q. Li, Y. Shen, Z. Ge, W. Zhang, S. Chen, Enhanced water-solubility, antibacterial activity and biocompatibility upon introducing sulfobetaine and quaternary ammonium to chitosan, Carbohyd. Polym. 143 (2016) 246-253.

[35] D. Zhu, H. Cheng, J. Li, W. Zhang, Y. Shen, S. Chen, Z. Ge, S. Chen, Enhanced water-solubility and antibacterial activity of novel chitosan derivatives modified with quaternary phosphonium salt, Mater. Sci. Eng. C 61 (2016) 79-84.

[36] Y. Su, L. Tian, M. Yu, Q. Gao, D. Wang, Y. Xi, P. Yang, B. Lei, P.X. Ma, P. Li, Cationic peptidopolysaccharides synthesized by 'click' chemistry with enhanced broad-spectrum antimicrobial activities, Polym. Chem. 8 (2017) 3788-3800.

[37] H. Ruihua, Y. Bingchao, D. Zheng, B. Wang, Preparation and characterization of a quaternized chitosan. J. Mater. Sci. 47 (2012) 845–851.

[38] Z.-X. Peng, L. Wang, L. Du, et al., Adjustment of the antibacterial activity and biocompatibility of hydroxypropyltrimethyl ammonium chloride chitosan by varying the degree of substitution of quaternary ammonium, Carbohydr. Polym. 81 (2010) 275–283.

[39] K. Suzuki, D. Oda, T. Shinobu, et al., New selectively n-substituted quaternary ammonium chitosan derivatives. Polym. J. 32 (2000) 334–338.

[40] C. Bangyekan, D. Aht-Ong, K. Srikulkit, Preparation and properties evaluation of chitosan-coated cassava starch films, Carbohydr. Polym. 63 (2006) 61–71.

[41] M.M. Hassan, Binding of a quaternary ammonium polymer-grafted-chitosan onto a chemically modified wool fabric surface: Assessment of mechanical, antibacterial and antifungal properties, RSC Adv. 5 (2015) 35497–35505.

[42] M. Lavertu, Z. Xia, A.N. Serreqi, et al., A validated ^{1}H NMR method for the determination of the degree of deacetylation of chitosan, J. Pharmaceut. Biomed. Anal. 32 (2003) 1149–1158.

[43] M.W. Anthonsen, O. Smidsrød, Hydrogen ion titration of chitosans with varying degrees of N-acetylation by monitoring induced 1H-NMR chemical shifts, Carbohyd. Polym. 26 (1995) 303–305.

[44] M. Rinaudo, P. Dung, C. Gey, M. Milas, Substituent distribution on O,N-carboxymethyl chitosan by 1H and 13C N.M.R., Int. J. Biol. Macromol. 14 (1992) 122–128.

[45] T.T.B. Nguyen, S. Hein, C.-H. Ng, W.F. Stevens, Molecular stability of chitosan in acid solutions stored at various conditions, J. Appl. Polym. Sci. 107 (2008) 2588–2593.

[46] D.J. Macquarrie, J.J.E. Hardy, Applications of functionalized chitosan in catalysis, Ind. Eng. Chem. Res. 44 (2005) 8499–8520.

[47] M. Ziegler-Borowska, D. Chełminiak, H. Kaczmarek, Thermal stability of magnetic nanoparticles coated by blends of modified chitosan and poly(quaternary ammonium) salt, J. Thermal Anal. Calorimetry 119 (2015) 499–506.

[48] J.B. Marroquin, K.Y. Rhee, S.J. Park, Chitosan nanocomposite films: Enhanced electrical conductivity, thermal stability, and mechanical properties. Carbohydr. Polym. 92 (2013) 1783–1791.

[49] I. Corazzari, R. Nisticò, F. Turci, et al., Advanced physicochemical characterization of chitosan by means of TGA coupled on-line with FTIR and GCMS: Thermal degradation and water adsorption capacity. Polym. Degrad. Stab. 112 (2015) 1–9.

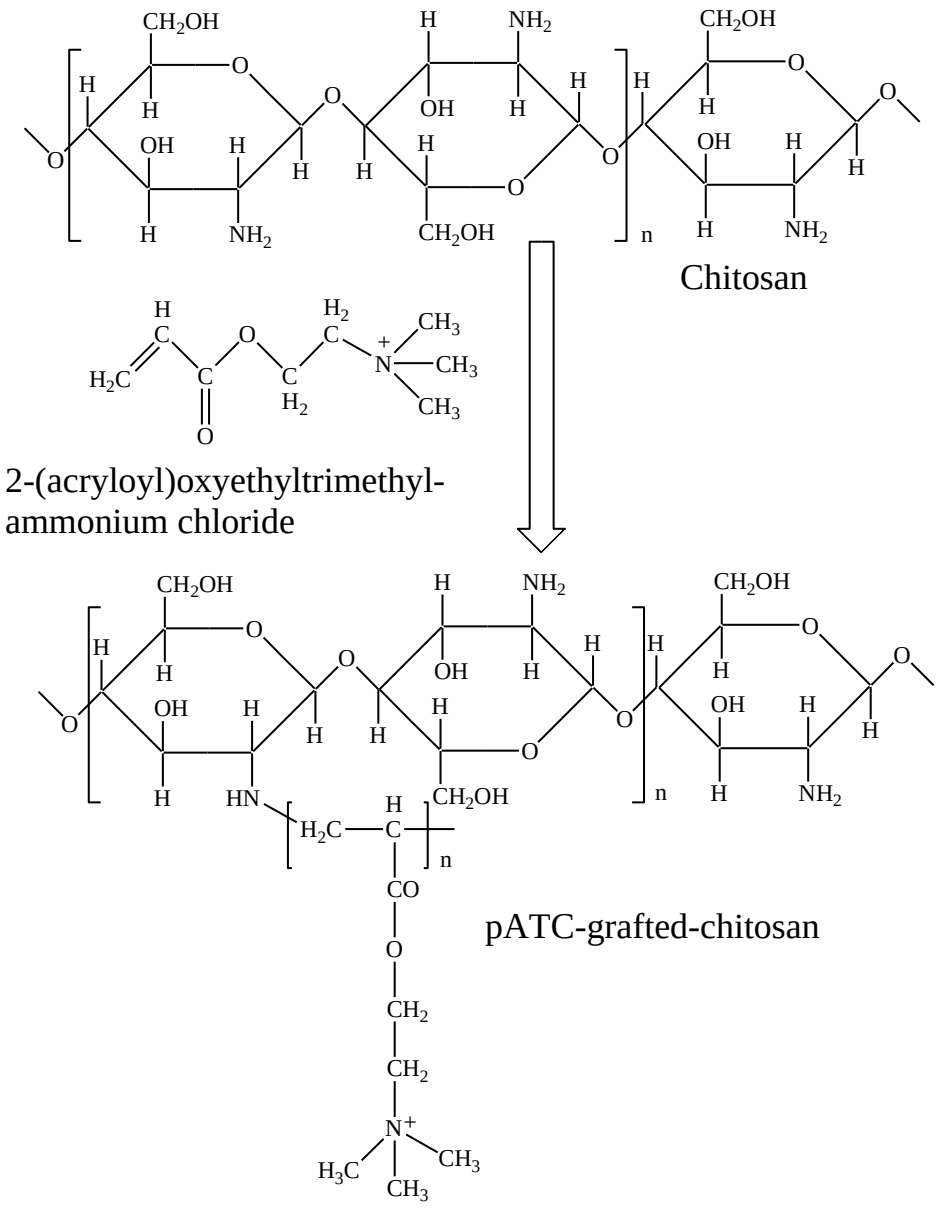

Fig. 1. Mechanism of grafting of pATC onto the macromolecular chain of chitosan.

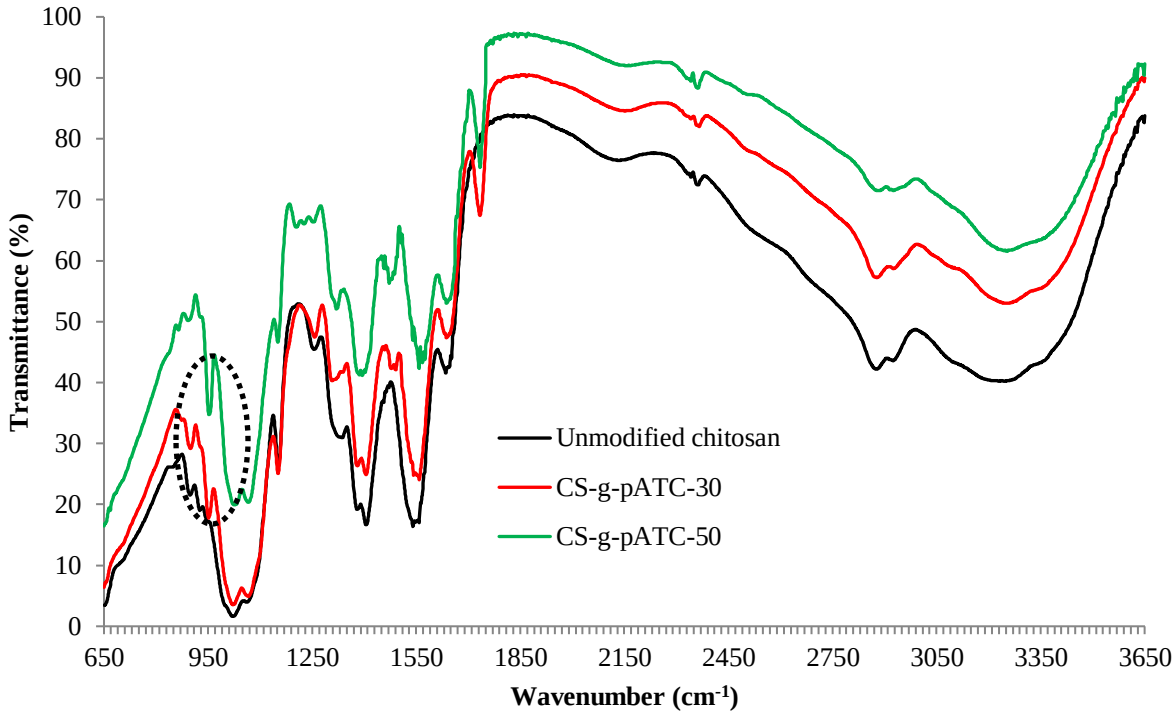

Fig. *2.* ATR-FTIR spectra of unmodified chitosan, CS-g-pATC-30 and CS-g-pATC-50.

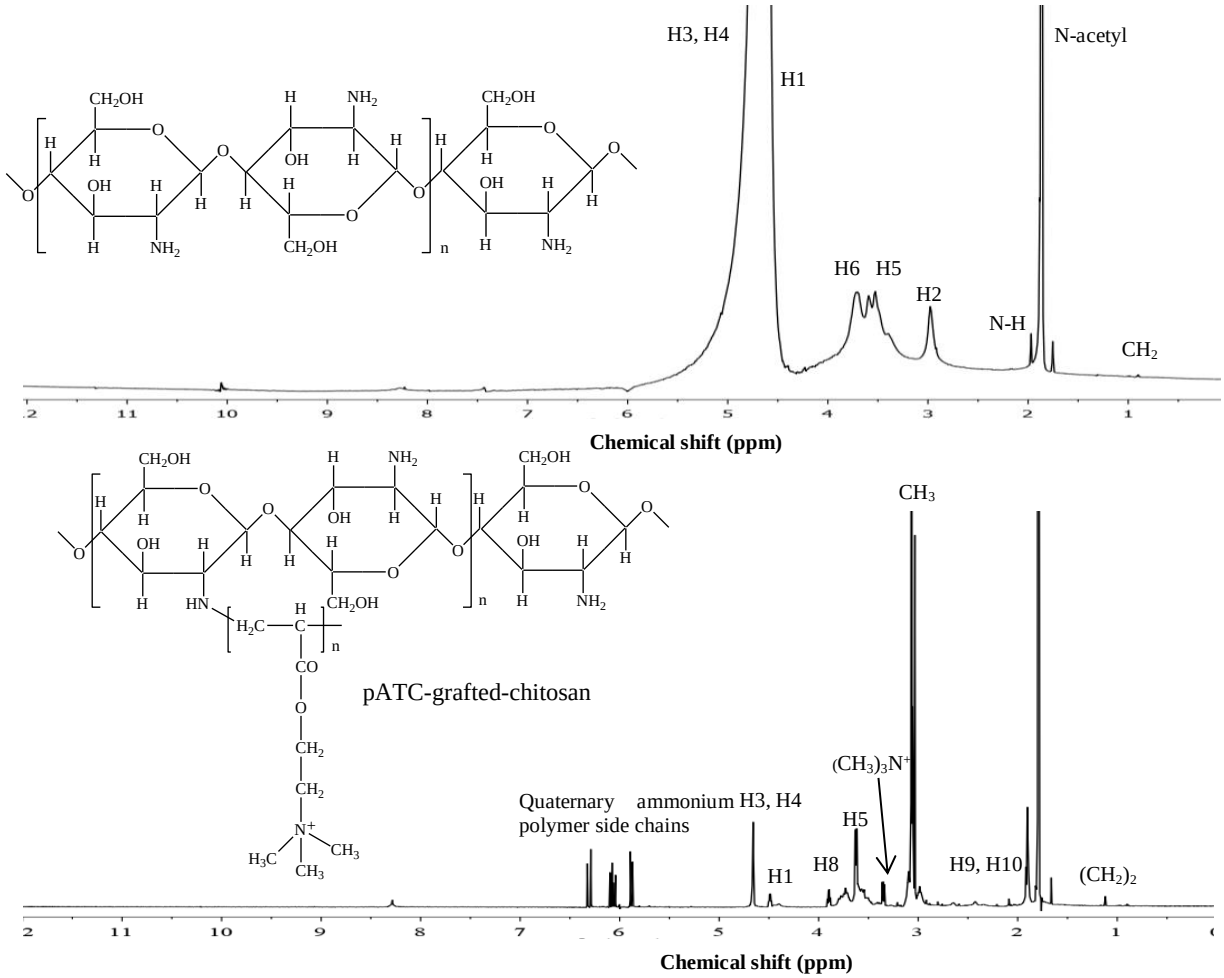

Fig. 3. ^{1}H-NMR spectra of (A) chitosan and (B) chitosan graft-copolymerized with 50% pATC.

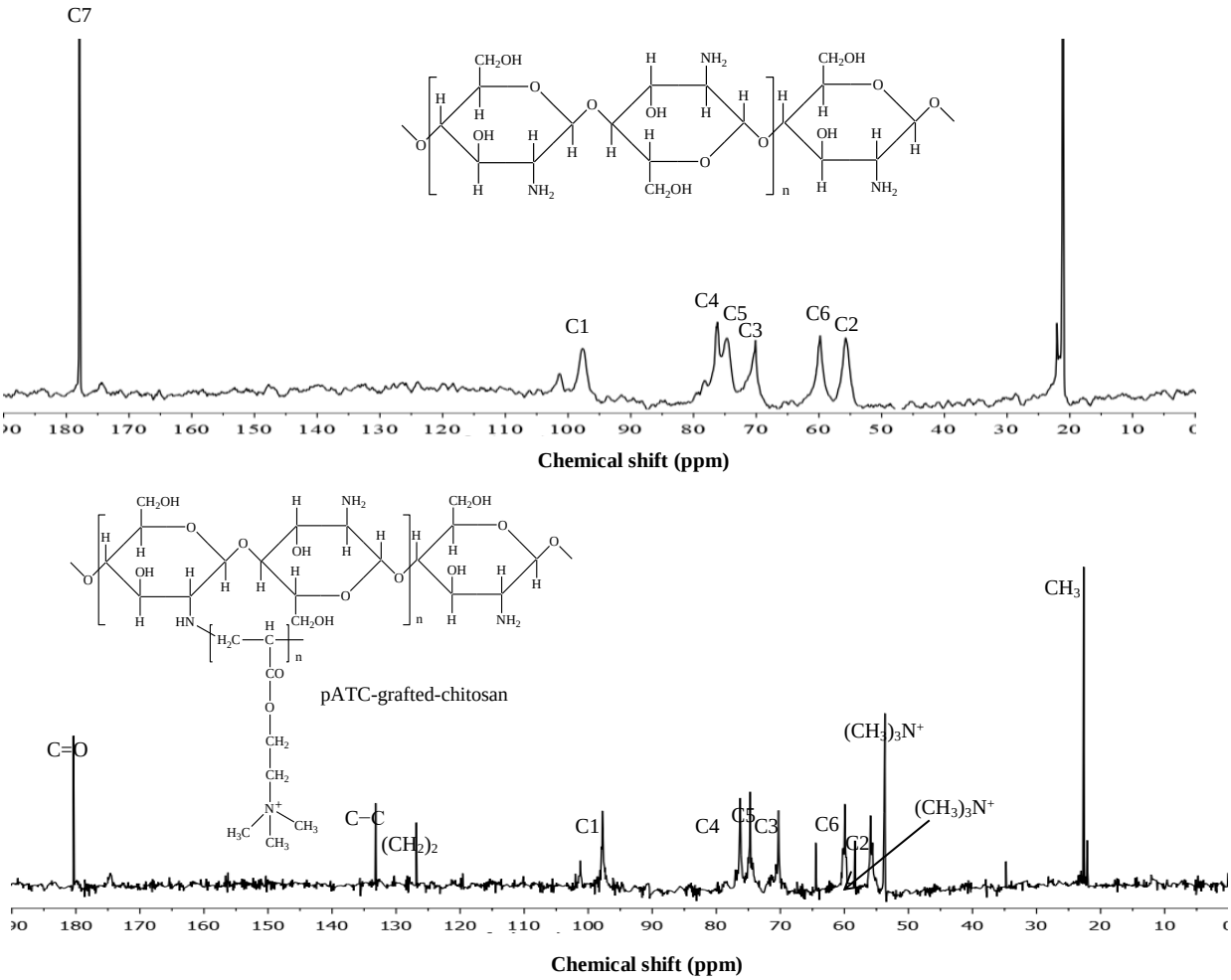

Fig. 4. ^{13}C-NMR spectra of (A) chitosan and (B) chitosan graft-copolymerized with 50% pATC.

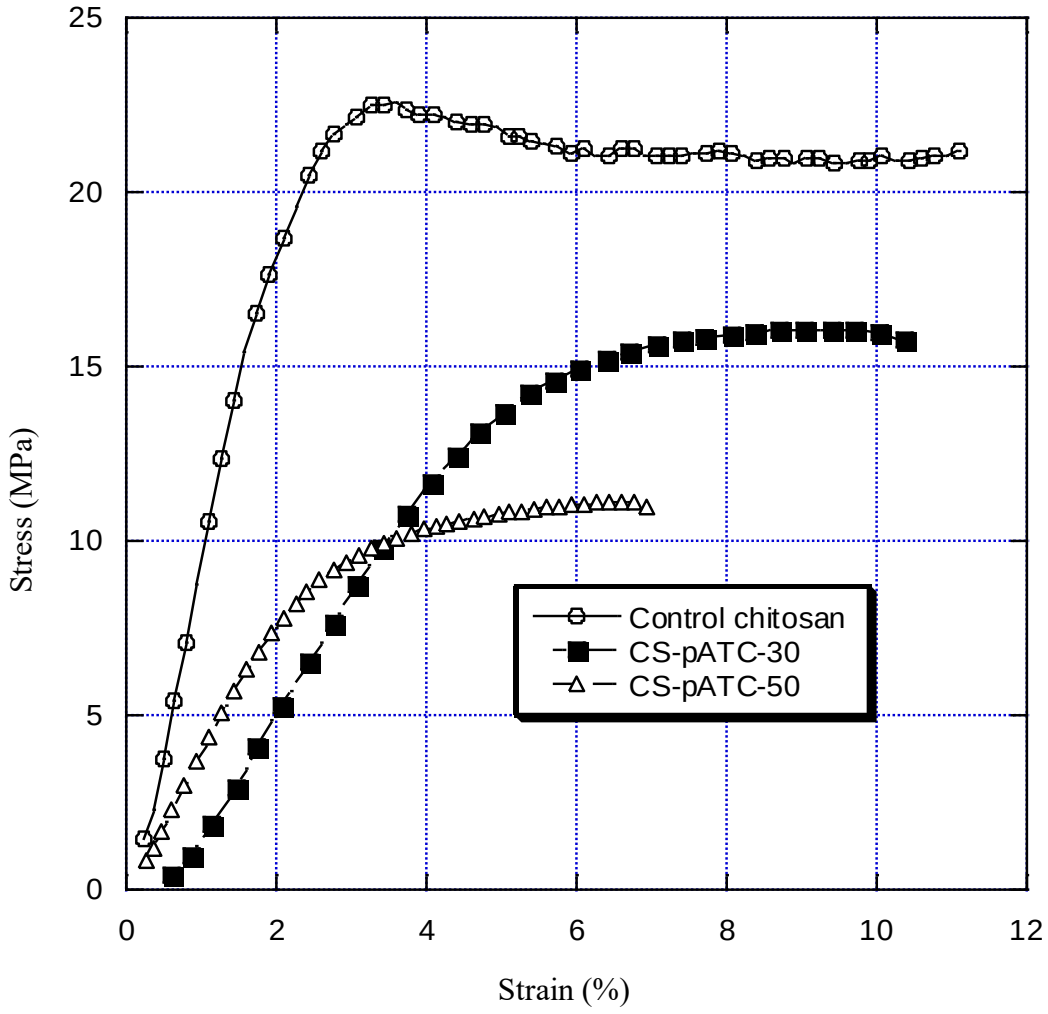

Fig. 5. Stress-strain curve of unmodified chitosan, CS-pATC-30, and CS-pATC-50 films.

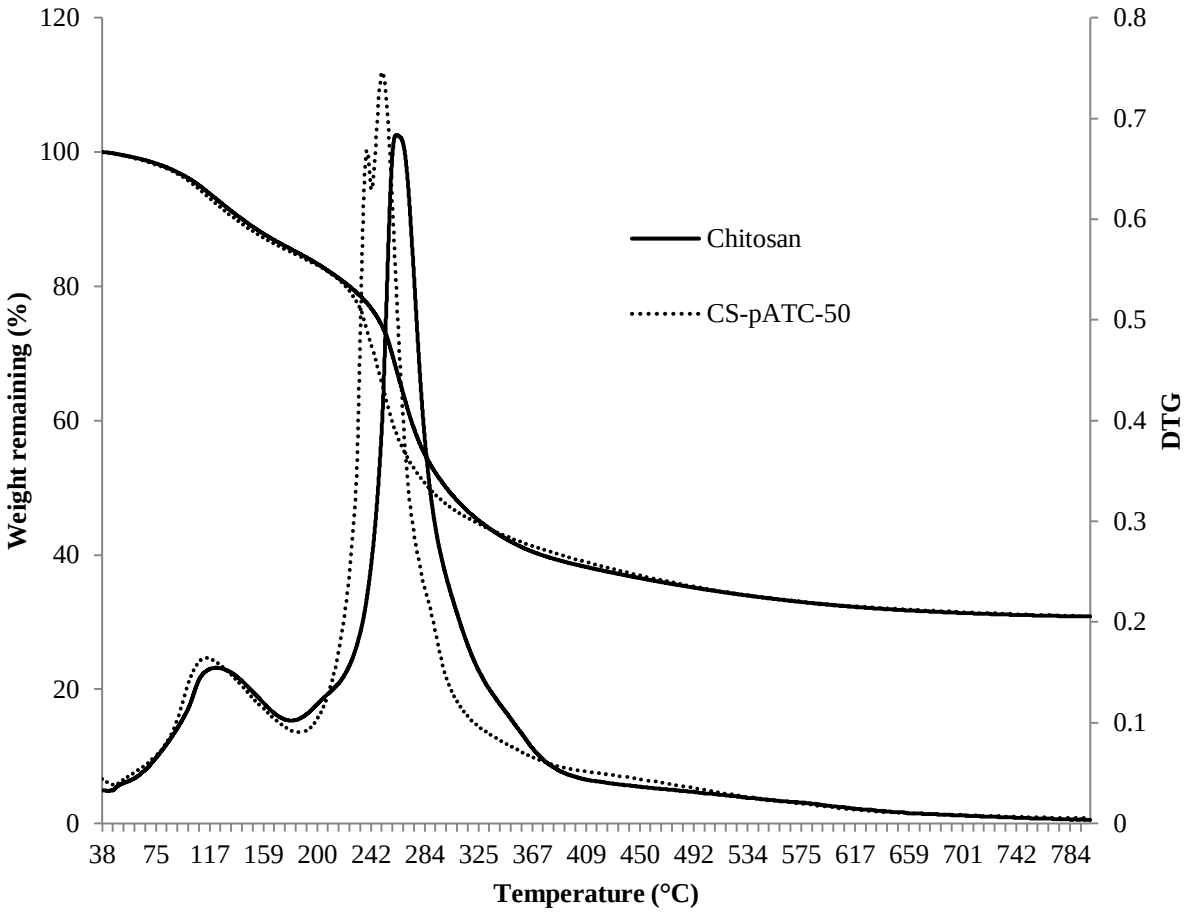

Fig. 6. TG and DTA curves of chitosan and CS-pATC-50 carried out under a nitrogen atmosphere at 10 °C/min heating rate.

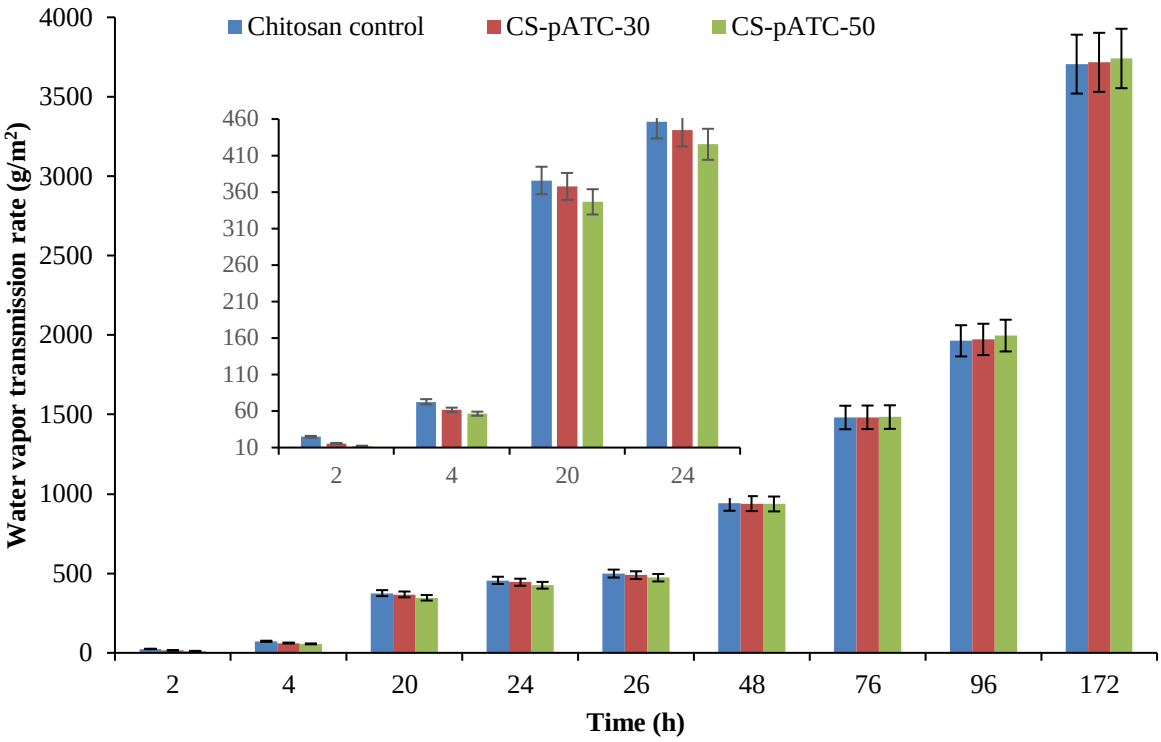

Fig. 7. The water vapor transmission rate of unmodified and pATC grafted chitosan films carried out at standard atmospheric conditions for 172 hours.

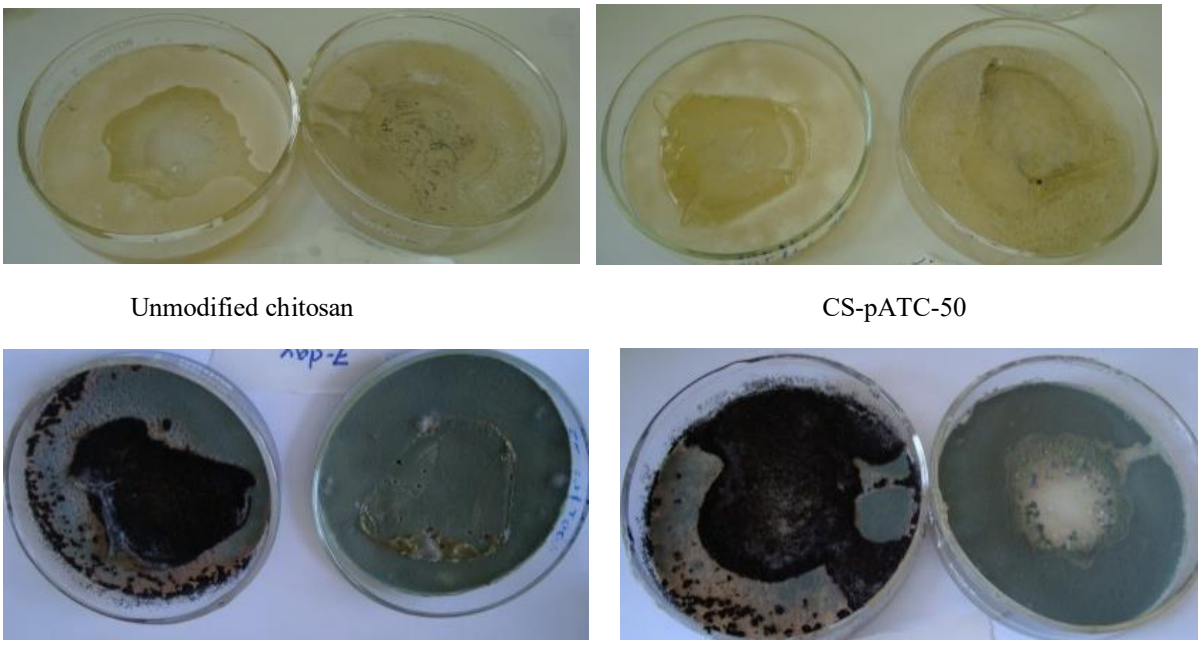

Fig. 8. Antimicrobial activities of unmodified chitosan and CS-pATC-50 against mixed *Aspergillus fumigatus* and *Aspergillus brasiliensis* (left) and *Aspergillus fumigatus* (right) after 2 (top) and 14 (bottom) days of incubation.

Supplementary Content.

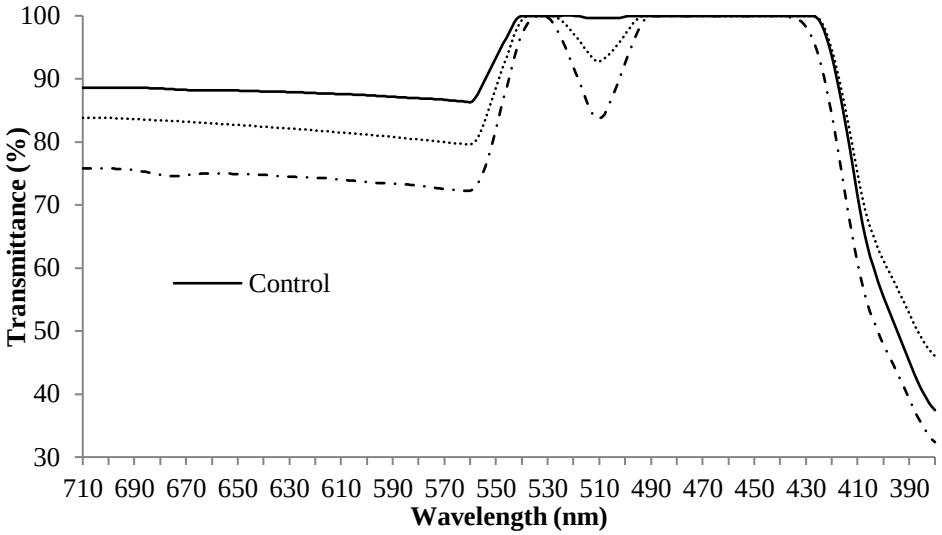

Fig. *S1*. Transparency of neat chitosan and pATC grafted chitosan films.

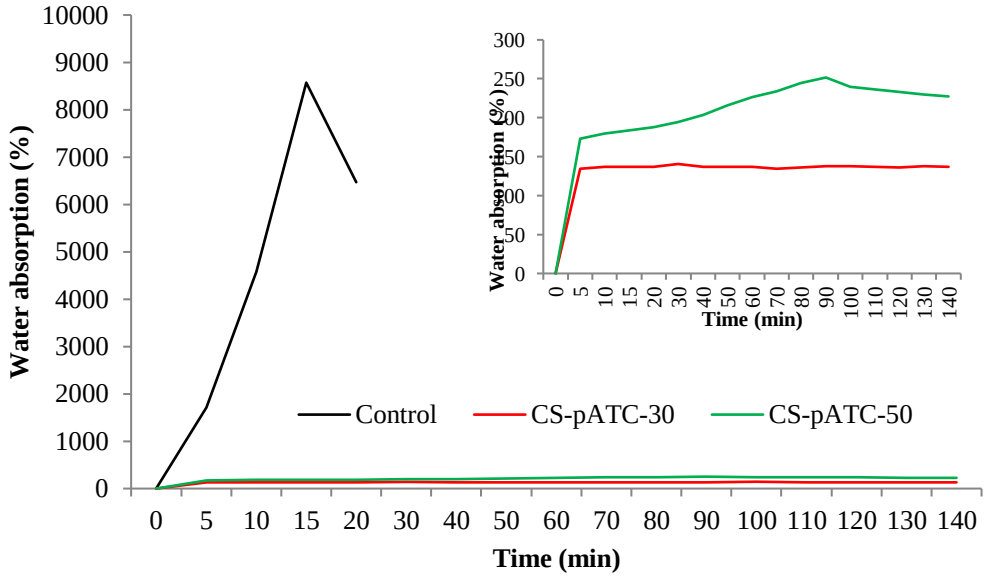

Fig. *S2*. The water absorption capacity of unmodified and pATC grafted chitosan films at the various times.

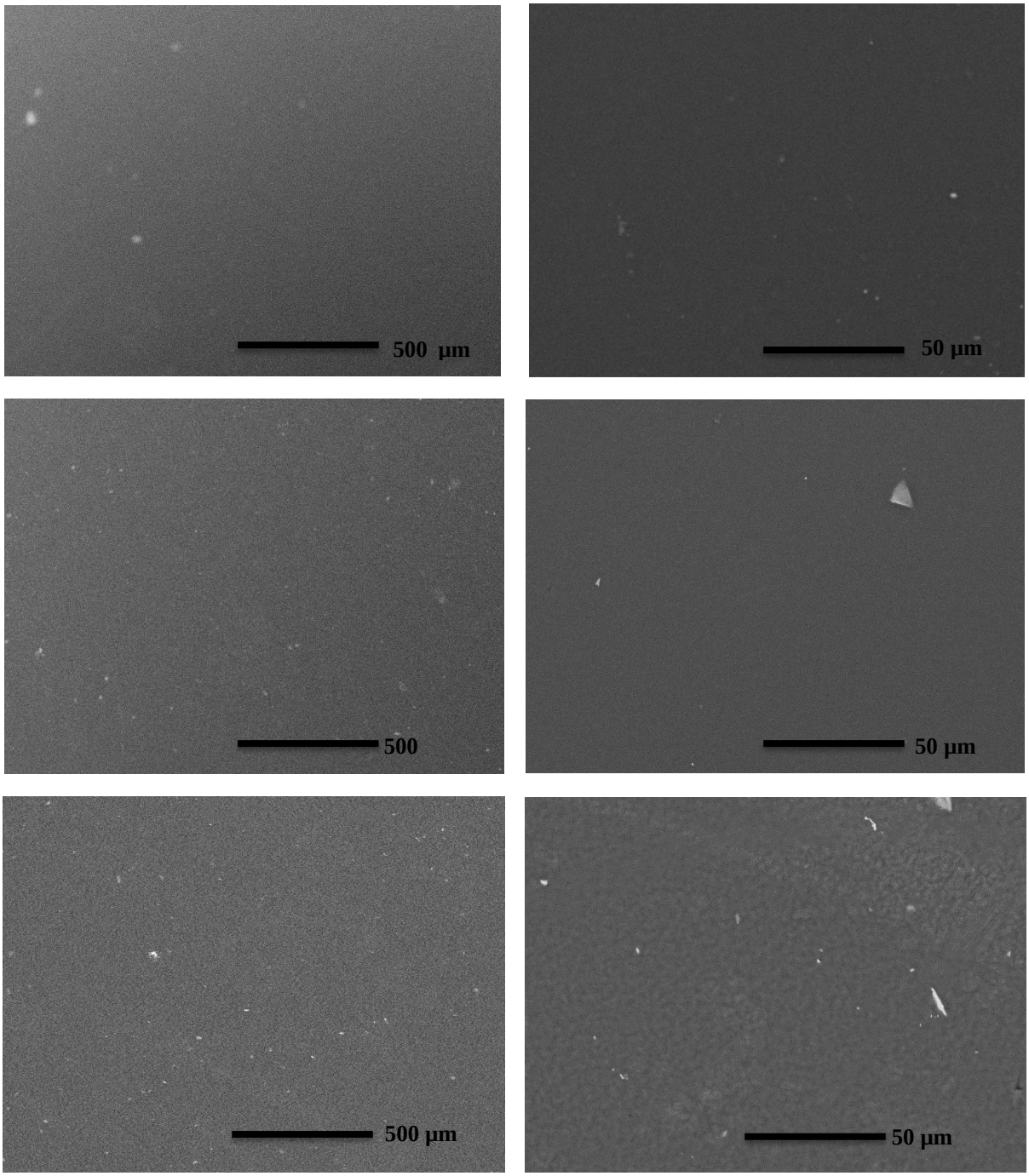

Figure *S3*. SEM images of surface of control (top), CS-pATC-30 (middle) and CS-pATC-50 (bottom) chitosan films.

Table S1

*CIE L*a*b** color values of control, CS-pATC-30, and CS-pATC-50 chitosan films

Sample ID.	*Average CIE L*a*b** color values		
	*L**	*a**	*b**
Unmodified chitosan	14.82±0.0.20	-0.15±0.10	0.14±0.10
CS-pATC-30	20.07±0.56	1.02±0.24	4.75±0.28
CS-pATC-50	25.95±1.61	5.18±1.18	6.33±0.65